3-D FDTD Design Simulation and Experimental Measurement of a Ka-Band Planar Antipodal Linearly-Tapered Slot Antenna (ALTSA)

Liang-Chen Kuo, *Student Member, IEEE*, Meng-Chung Tsai, *Student Member, IEEE*, and Huey-Ru Chuang, *Member, IEEE*

***Abstract*—Three-dimensional (3-D) finite-difference time-domain (FDTD) simulation of a planar broadband Ka-band (25–35 GHz) antipodal linearly-tapered slot antenna (ALTSA) and the experimental measurements are presented. The Berenger perfectly matched layer (PML) absorbing boundary condition is used for the FDTD computation. A printed ALTSA has been realized by using the RT/Duroid PCB substrate. Good agreement between simulation and measurement were achieved.**

***Index Terms*—ALSTA, antipodal linearly-tapered slot, FDTD, Ka-band antenna.**

I. Introduction

THE broadband and high-gain natures of tapered slot antennas (TSAs) have been reported for years. Due to its coplanar structure, the TSA is easily integrated with microwave integrated circuits. In [1], some parameters that affect the performance of the TSA, such as the thickness of the substrates and the profile of the tapered slot, were presented by Yngvesson *et al.* R. Janaswamy and D. H. Schaubert [2] proposed a good-stepped approximation to analyze the TSA with exponential taper profiles, which are the general cases of TSAs. Nevertheless, the conventional feeding technologies applied in TSAs including CPW-to-slot transition, coax-to-slot transition, or even finline feeds, all face on difficulty of impedance matching. To surmount the impedance matching difficulty, TSA of antipodal geometry was introduced [3]. The antipodal linearly-tapered slot antenna (ALTSA) reported in [4], [5] describes the development and performance of a balanced antipodal Vivaldi antenna. It can produce an ultrawide bandwidth element for circuit integration. One of the advantages of the antipodal geometry is that no stubs are need on the PCB to achieve impedance matching.

For the design simulation of TSAs, rigorous numerical modeling of the complete planar ALTSA structure has yet to be studied. In this paper, 3-D finite-difference time-domain (FDTD) method was employed to simulate the complete structure of a planar Ka-band ALTSA. A printed ALTSA has been realized by using the RT/Duroid PCB substrate. Numerical results and measured data are compared.

Manuscript received March 5, 2001; revised July 2, 2001. The review of this letter was arranged by Associate Editor Dr. Arvind Sharma.

The authors are with the Department of Electrical Engineering, National Cheng Kung University, Tainan, Taiwan, R.O.C (e-mail: chuangh@eembox.ee.ncku.edu.tw).

Publisher Item Identifier S 1531-1309(01)08081-3.

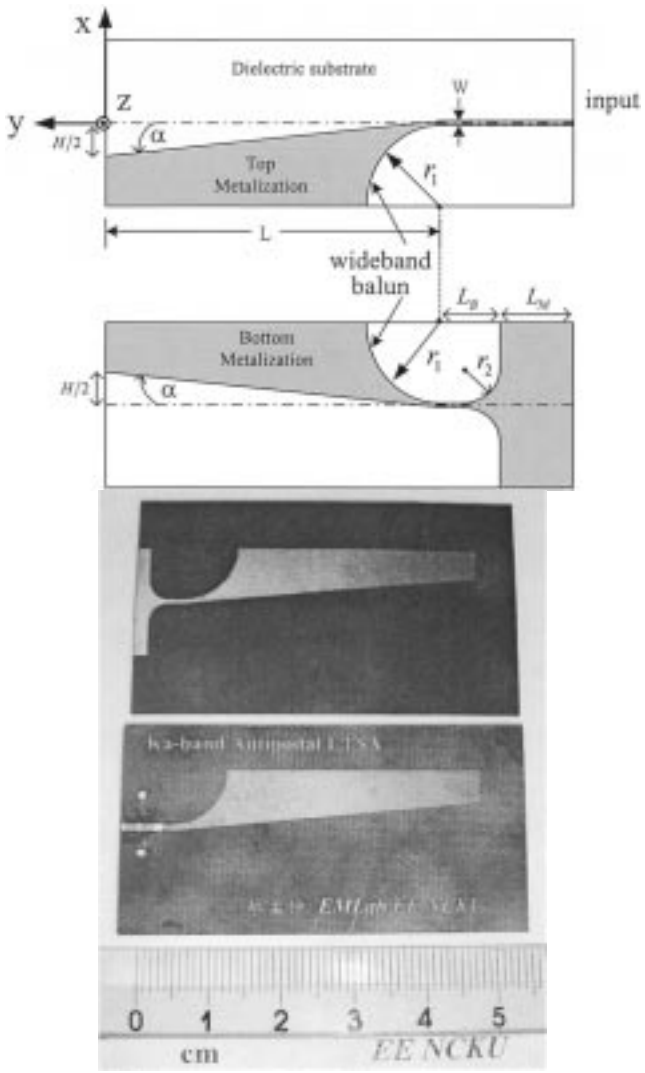

Fig. 1. Geometry of an ALTSA and photograph of realized Ka-band printed ALTSAs on a RT/Duroid substrate.

II. ALTSA Geometry Description

The geometry and photograph of realized Ka-band (25–35 GHz) planar printed ALTSAs is shown in Fig. 1. The top metallization of the ALTSA starts from a feeding microstrip line and gradually flared with an angle α. The bottom metallization consists of a ground plane of the feeding microstrip and is also

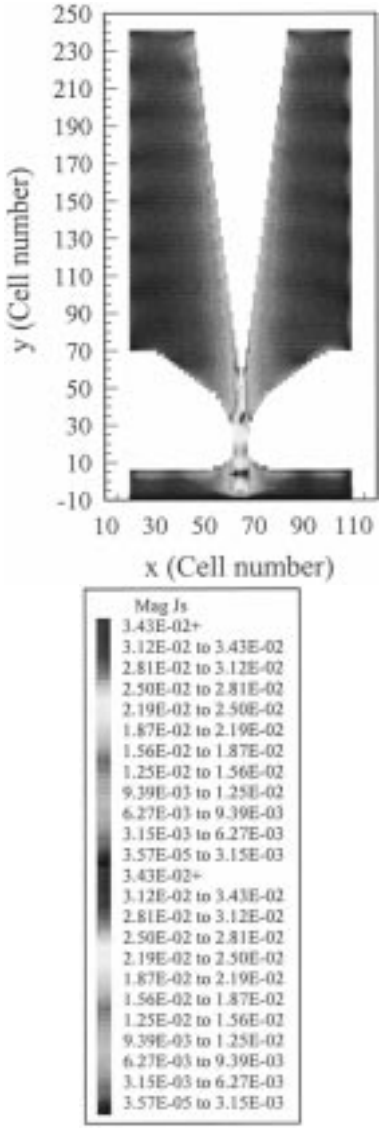

Fig. 2. Computed surface current distribution on the metal plates of a printed Ka-band ALTSA at 30 GHz.

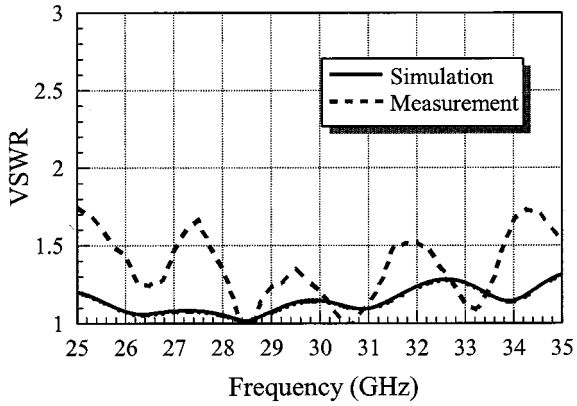

Fig. 3. VSWR of a printed Ka-band ALTSA antenna: FDTD simulation and measurement.

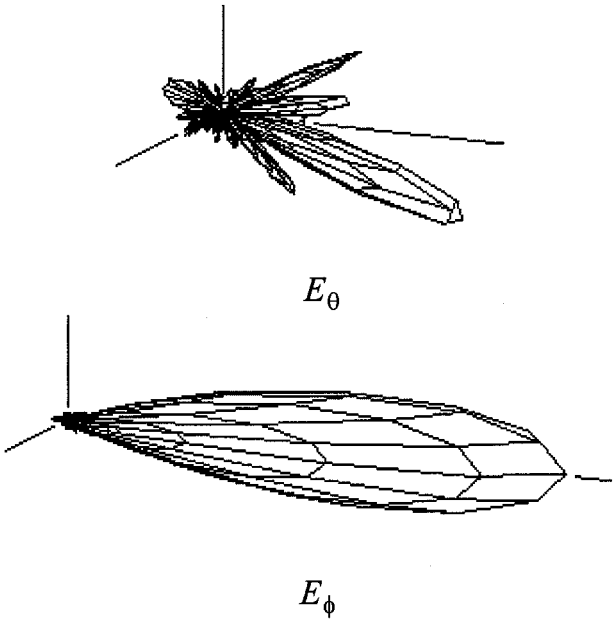

Fig. 4. Computed 3-D E_θ and E_ϕ radiation patterns of a printed Ka-band ALTSA at 30 GHz.

flared to the symmetrical side of the top metallization with the same angle α. The arcs with radius r_1 on the top and bottom metallization are tunable to make the microstrip line smoothly connected to the tapered-slot antenna section without discontinuities. It can render broadband impedance matching. As for the arcs with radius r_2 on the bottom metallization, they can be arbitrarily chosen to make the feeding section changed from unbalanced to balanced structure. The feed structure is essentially a broadband balun. Referring to the empirical design rules in [6], [7], the structure parameters are listed as follows.

- PCB Substrate: RT/Duroid 5880 (0.508 mm thickness, $\varepsilon_r = 2.2$, $\tan\delta = 0.0009$).
- Antenna length: $L = 43$ mm (about 4.3λ at 30 GHz).
- Flare angle: $2\alpha = 11^o$.
- Feeding microstrip line : length $(L_{\rm B} + L_{\rm M}) = 7$ mm, width $w = 1$ mm.
- Radii of the arcs: $r_1 = 7.75$ mm, $r_2 = 2$ mm.

Note that r_1 and r_2 are tunable to make the microstrip line smoothly connected to the ALTSA without any discontinuities.

III. 3-D FDTD Simulation Results and Measurement

In order to ensure the accuracy of the computed results, here the FDTD cell resolution is small than 1/20 wavelength at the highest frequency (35 GHz). The computation volume is $(120\Delta x \times 260\Delta y \times 40\Delta z)$ cells with the cell size $\Delta x = \Delta y = 0.2\,$mm and $\Delta z = 0.127\,$mm.

The Berenger perfectly matched layer (PML) absorbing boundary condition is used for the FDTD computation [8]. Here the PML-ABC layer adopts ten cells. To obtain multiple frequencies with only one FDTD run, a Gaussian pulse is selected by specifying the z direction excitation source within the coordinates $(i_s\Delta x,\ j_s\Delta y,\ k_s\Delta z)$ of the source location at time step $n\Delta t$ as follows:

$$E^n_{in,z}(i_s, j_s, k_s) = E_o \exp\left[-\frac{\left(t - t_0 - \frac{(y-y_0)}{\nu}\right)^2}{T^2}\right]. \quad (1)$$

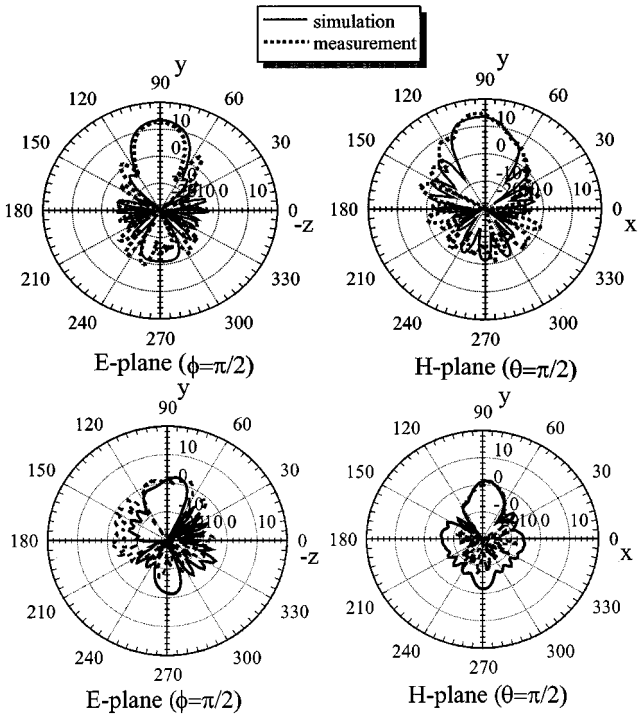

Fig. 5. Co- and cross-polarization 2-D radiation patterns of a printed Ka-band ALTSA at 30 GHz: FDTD simulation and measurement (directivity $= 14.6$ dB).

The pulse has the maximum value at $y = y_0$ when $t = t_0$ (ν is the velocity of the pulse in the substrate medium). Its Fourier transform is still of Gaussian shape. The parameter $T (= 10\Delta y/\sqrt{3}\nu)$ is determined from the pulse width (chosen to be approximately $20\Delta y$) defined to be the width between the two symmetric points which have 5% ($= e^{-3}$) of the maximum value of the pulse [9]. E_o is set to be equal to unity.

Through time-domain to frequency-domain transformation, we can obtain the surface current distribution on the metal plates of the antenna. This distribution can obtain directly from the tangential magnetic fields in spectral-domain. By using the near-field data obtained in a single FDTD run, the near-to-far-field transformation is used to calculate the complete far-field response or the radiation pattern of an antenna.

Fig. 2. shows the computed surface current distribution on the metal plates of a printed Ka-band ALTSA at 30 GHz. It can be observed that the surface current is mainly distributed along the inner side of the plates. The computed and measured VSWR are shown in Fig. 3. The VSWR is approximately lower than 1.5 from 27 to 32 GHz due to broadband characteristics. Fig. 4. shows computed 3-D E_θ and E_ϕ radiation patterns of the ALTSA at 30 GHz. Fig. 5 shows the computed and measured H-plane and E-plane antenna patterns of the ALTSA at 30 GHz. Satisfactory agreement is observed in the main-beam region. The antenna directivity of the ALTSA is about 14.5 dBi, which agrees well with that from FDTD simulation.

IV. Conclusion

This paper presents 3-D FDTD design simulation of the complete structure and experimental measurements of a Ka-band planar printed microstrip-fed ALTSA. The Berenger PML-ABC is used for FDTD computation. An ALTSA is fabricated on a RT/Duroid substrate. Good agreement between numerical and measured results on input return loss and antenna directivity has been achieved. The input VSWR of the realized ALTSA is lower than 1.5 (27 GHz $\sim$ 32 GHz) and the antenna directivity is about 14.5 dBi at 30 GHz. The developed ALTSA could be a good choice for the antennas used in the Ka-band LMDS (local multipoint distributed systems).

References

[1] K. S. Yngvesson, D. H. Schaubert, and E. L. Kollberg *et al.*, "Endfire tapered slot antennas on dielectric substrates," *IEEE Trans. Antennas Propagat.*, vol. AP-33, pp. 1392–1400, Dec. 1985.

[2] R. Janaswamy and D. H. Schaubert, "Analysis of the tapered slot antenna," *IEEE Trans. Antennas Propagat.*, vol. AP-35, pp. 1058–1065, Sept. 1987.

[3] E. Gazit, "Improved design of the vivaldi antenna," *Proc. Inst. Elect. Eng. H*, vol. 135, no. 2, pp. 89–92, Apr. 1988.

[4] R. N. Simons, R. Q. Lee, and T. D. Perl, "Non-Planar linearly tapered slot antenna with balanced microstrip feed," in *IEEE AP-S Int. Symp.*, vol. 4, Chicago, IL, 1992, pp. 2109–2112.

[5] J. D. S. Langley, P. S. Hall, and P. Newham, "Balanced antipodal vivaldi antenna for wide bandwidth phased arrays," in *Proc. IEEE Microwave Antenna Propagat.*, vol. 143, Apr. 1996, pp. 97–102.

[6] K. S. Yngvesson *et al.*, "The tapered slot antenna- a new integrated element for millimeter-wave applications," *IEEE Trans. Microwave Theory Tech.*, vol. MTT-37, pp. 365–374, Feb. 1989.

[7] C. Wu, L. Shen, G.-Y. Deng, Y. Shen, and J. Litva, "Experimental study of a wide band LTSA which is fed by an Inverted Microstrip Line (IML)," in *IEEE Antennas Propagat. Soc. Int. Symp.*, vol. 4, 1998, pp. 2328–2331.

[8] J.-P. Berenger, "A perfectly matched layer for the absorption of electromagnetic waves," *J. Comput. Phys.*, vol. 114, pp. 185–200, 1994.

[9] X. Zhang and K. K. Mei, "Time-domain finite difference approach to the calculation of the frequency-dependent characteristics of microstrip discontinuities," *IEEE Trans. Microwave Theory Tech.*, vol. 36, pp. 1775–1787, Dec. 1988.